Marine Pollution Bulletin 118 (2017) 213–220

Contents lists available at ScienceDirect

Marine Pollution Bulletin

journal homepage: www.elsevier.com/locate/marpolbul

The acclimation process of phytoplankton biomass, carbon fixation and respiration to the combined effects of elevated temperature and pCO_2 in the northern South China Sea

Guang Gao [a,b], Peng Jin [a], Nana Liu [a], Futian Li [a], Shanying Tong [a], David A. Hutchins [c], Kunshan Gao [a,*]

[a] State Key Laboratory of Marine Environmental Science, Xiamen University, Xiamen 361005, China
[b] Marine Resources Development Institute of Jiangsu, Huaihai Institute of Technology, Lianyungang 222005, China
[c] Marine Environmental Biology, Department of Biological Sciences, University of Southern California, 3616 Trousdale Parkway, Los Angeles, CA 90089, USA

ARTICLE INFO

Article history:
Received 5 January 2017
Received in revised form 21 February 2017
Accepted 22 February 2017
Available online 1 March 2017

Keywords:
Ocean acidification
Ocean warming
Photosynthesis
Primary productivity
Respiration
South China Sea

ABSTRACT

We conducted shipboard microcosm experiments at both off-shore (SEATS) and near-shore (D001) stations in the northern South China Sea (NSCS) under three treatments, low temperature and low pCO_2 (LTLC), high temperature and low pCO_2 (HTLC), and high temperature and high pCO_2 (HTHC). Biomass of phytoplankton at both stations were enhanced by HT. HTHC did not affect phytoplankton biomass at station D001 but decreased it at station SEATS. HT alone increased net primary productivity by 234% at station SEATS and by 67% at station D001 but the stimulating effect disappeared when HC was combined. HT also increased respiration rate by 236% at station SEATS and by 87% at station D001 whereas HTHC reduced it by 61% at station SEATS and did not affect it at station D001. Overall, our findings indicate that the positive effect of ocean warming on phytoplankton assemblages in NSCS could be damped or offset by ocean acidification.

1. Introduction

From 1979 to 2012, the mean global sea surface temperature (SST) increased at a rate of ~0.12 °C per decade (IPCC, 2013). Particularly, the warming rate in the surface of South China Sea (~0.26 °C per decade) from 1982 to 2004 (Fang et al., 2006) appears to be about 2 times faster. It is extremely likely that more than half of the observed increase in global average surface temperature from 1951 to 2010 was caused by the anthropogenic increase in greenhouse gas concentrations and other anthropogenic forcings. Ocean warming is projected to rise approximately by 0.6 °C (Representative Concentration Pathway (RCP) 2.6) to 2.0 °C (RCP 8.5), in the upper 100 m of the water column by the end of the 21st century (IPCC, 2013).

Ocean warming is known to affect primary productivity both directly and indirectly. In situ surface chl *a* declined exponentially with rise of SST (13–23 °C) in the northeast Atlantic Ocean from latitudes 29 to 63° N in spring and summer, which was attributed to enhanced stratification and consequent reduced upward transport of nutrients into the upper mixed layer (Poll et al., 2013). The seawater volume-specific primary productivity also decreased with temperature rise due to lower phytoplankton biomass (Poll et al., 2013). Mesocosm experiments have also demonstrated that ocean warming (an increase of 6 °C) can decrease phytoplankton biomass by ~80% in the Baltic Sea (Sommer et al., 2015). On the other hand, ocean warming did not affect volume-specific primary productivity in the Baltic Sea (Lewandowska et al., 2012).

The oceans have absorbed approximately 30% of the emitted anthropogenic carbon dioxide (IPCC, 2013). Such a dissolution of CO_2 increases seawater CO_2 partial pressure and bicarbonate ion levels and decreases pH and carbonate ion concentrations, leading to ocean acidification (Orr et al., 2005). By 2100, the projected decline in global-mean surface pH is projected to be approximately 0.065 for RCP2.6, 0.145 for RCP4.5, 0.203 for RCP6.0, and 0.31 for RCP8.5 (IPCC, 2013). In terms of the South China Sea, an accelerated trend of ocean acidification has been reported and the rate of pH decline almost tripled between 1951 and 2000, compared to that between 1840 and 1950 (Liu et al., 2014).

Dissolved CO_2 may be a potentially limiting factor for marine primary productivity because of the low CO_2 level in seawater and the low affinity of the enzyme Rubisco for dissolved CO_2 (Falkowski and Raven, 2013). In addition, CO_2 in seawater diffuses approximately 10,000 times slower than in air, leading to its supply rate being much lower than the demand of photosynthetic carbon fixation (Raven, 1993; Riebesell et al., 1993). Although phytoplankton have evolved carbon-concentrating mechanisms (CCMs) to cope with these challenges (Giordano et al., 2005; Reinfelder, 2011; Raven et al., 2012), increased CO_2 concentration may still be beneficial since energy saved due to down-regulation of CCMs under elevated CO_2 can be utilized in other

* Corresponding author.
E-mail address: ksgao@xmu.edu.cn (K. Gao).

http://dx.doi.org/10.1016/j.marpolbul.2017.02.063
0025-326X/

metabolic processes (Wu et al., 2010). Early laboratory and shipboard experiments suggested that increased CO_2 indeed could enhance phytoplankton growth rates and thus marine primary productivity (Riebesell et al., 1993; Hein and Sand-Jensen, 1997; Schippers et al., 2004). Since then, neutral effects of increased CO_2 on growth of phytoplankton assemblages have also been reported (Gao et al., 2012a, 2012b and references therein). Furthermore, ocean acidification can even reduce primary productivity of surface phytoplankton assemblages when exposed to incident solar radiation (Gao et al., 2012b). Therefore, the effects of ocean acidification on marine primary productivity remain controversial and its interactions with other environmental factors, such as warming, solar UV radiation, hypoxia, etc. are incompletely understood (Gao et al., 2012a; Häder and Gao, 2015; Mostofa, 2016).

Ocean warming and acidification, both caused by increasing atmospheric CO_2, are proceeding simultaneously. The interactive or combined effects of warming and OA could be completely different from that of either one stressor (Hare et al., 2007; Feng et al., 2009; Gao et al., 2012a; Tatters et al., 2013). Several oceanographic cruises and ship board experiments in the European sector of the Arctic Ocean, showed that gross primary production increased with pCO_2 (145–2099 μatm) and the greatest increase was observed in lower temperature regions, indicating CO_2-enhanced primary production in the European Arctic Ocean is temperature-dependent (Holding et al., 2015).

The South China Sea (SCS) is located between the equator and 23.8° N, from 99.1 to 121.1° E, and is one of the largest marginal seas in the world, with a total area of about 3.5×10^6 km^2. Therefore, understanding the effects of ocean warming and acidification on primary production in SCS would help us to define the role of marginal seas in the global carbon cycle. However, only a very few studies on the effects of ocean acidification or warming on primary productivity in the SCS have been reported. Wu and Gao (2010) reported that CO_2 enrichment (700 μatm) did not affect the photosynthetic carbon fixation rate of phytoplankton at a near-shore site in SCS, compared to the ambient CO_2 level (380 μatm). Gao et al. (2012b) demonstrated that increased pCO_2 (800 or 1000 μatm) reduced primary productivity in off-shore stations of the SCS. Therefore, we hypothesized that the effects of ocean acidification or/and warming on primary productivity in SCS would be site-dependent. None of the previous studies have examined co-effects of warming and increased CO_2 on primary production in the SCS. In this study, to test this hypothesis we conducted shipboard microcosm experiments at both near-shore and off-shore stations to determine the combined effects of ocean warming and acidification on biomass, photosynthetic carbon fixation, and dark respiration of phytoplankton assemblages in the SCS.

2. Methods

2.1. Experimental setup

The experiments were conducted at one off-shore station SEATS (17.9963° N, 115.9621° E) and one near-shore station D001 (18.9740° N, 110.7166° E) in the NSCS (Fig. 1). Surface seawater (0–2 m) was collected before sunrise with a 10 L acid-cleaned plastic bucket, filtered (180 μm) to remove large grazers and dispensed into nine microcosms. Microcosms consisted of cylindrical polymethyl methacrylate tanks (32 L, 0.34 m water depth) with water-jacketed space for circulating cooled water. In the microcosms, phytoplankton assemblages could be exposed to 81–91% and 64–91% of full sunlight at the off-shore and near-shore stations respectively, due to the shielding of the cover, water-jacket and the depth of the water. Two levels of temperature (in situ, in situ + 3 °C) and pCO_2 (ambient, ambient + 610 μatm) were used. There were three triplicated treatments: low temperature and low pCO_2, LTLC; high temperature and low pCO_2, HTLC; high temperature and high pCO_2, HTHC. The treatment of low temperature and high pCO_2 was missing due to the lack of microcosms. Microcosm temperature was controlled and monitored via circulating coolers with a

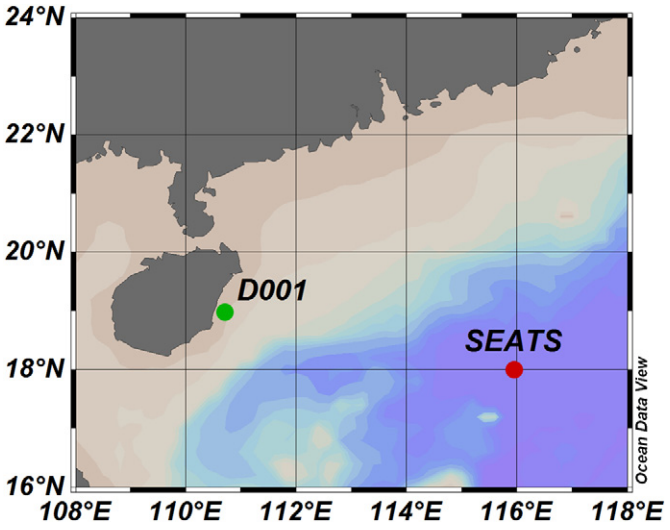

Fig. 1. Experimental stations in the northern South China Sea.

variation of ± 1.0 °C (CTP-3000, EYELA, Japan) and stable CO_2 equilibrium with the sea water (variation of pCO_2 < 5%) was achieved within 24 h using a CO_2 enricher (CE-100, Wuhan Ruihua Instrument & Equipment Ltd., China). The CO_2 enricher mainly comprises of a chamber, a mixer, a CO_2 meter, a pump, a screen, an outlet and two inlets. The two inlets are connected to ambient air and pure CO_2 respectively. The valve connected to the pure CO_2 inlet is switched off when the CO_2 level achieve the set value, and it is switched on when the CO_2 level is <95% of the set value. The screen can show the real-time CO_2 level and the gas could be transported into the incubation tanks by the pump. This system ensures that the CO_2 enricher could supply stable pCO_2 and monitor the pCO_2 level continuously (Fig. S1). To make sure the output pCO_2 equaling to the pCO_2 in seawater in the incubation tanks, we used an automated flow-through pCO_2 measuring system (Model 8050, GO, USA) to examine and calibrate the CO_2 enricher before the experiment. The incubations were conducted for seven days for station SEATS (Aug 3rd–9th 2012) and six days for station D001 (Aug 14th–19th 2012). We planned to conduct the same incubation period for both stations, but the incubation at station D001 was terminated one day earlier than the planned date due to a typhoon.

2.2. Solar radiance

The incident solar radiation was continuously monitored using an Eldonet broadband filter radiometer (Eldonet XP, Real Time Computer, Germany) that was fixed at the top of the ship. It measured every second and recorded the means over each minute.

2.3. Carbonate chemistry parameters

The seawater pH in the microcosm was recorded with a pH meter (FE20, Mettler Toledo, Greifensee, Switzerland) every hour during the first day of incubation and daily afterwards. The pCO_2 in seawater was maintained with the CO_2 enricher and measured by an automated flow-through pCO_2 measuring system (Model 8050, GO, USA). Other carbonate system parameters were derived via CO2SYS (Pierrot et al., 2006), using the equilibrium constants of K_1 and K_2 for carbonic acid dissociation (Roy et al., 1993).

2.4. Chlorophyll a analysis

For the measurement of chlorophyll *a* (chl *a*), 500 mL of seawater were filtered onto a Whatman GF/F glass fiber filter (25 mm). Then the filter was placed in 5 mL 93% acetone at −20 °C for 24 h. Chl *a*

Table 1
The daytime (12 h) mean solar radiation (PAR, μmol photons m^{-2} s^{-1}) during incubation at off-shore station SEATS and near-shore station D001.

SEATS		D001	
Date	Solar radiation	Date	Solar radiation
03/08/2012[a]	1454	14/08/2012[a]	1512
04/08/2012	1304	15/08/2012	1480
05/08/2012	1146	16/08/2012	400
06/08/2012	1113	17/08/2012	111
07/08/2012	927	18/08/2012	1520
08/08/2012	1592	19/08/2012	1583
09/08/2012	1582	20/08/2012[b]	1346
10/08/2012[b]	1381	Mean[c]	1136
Mean[c]	1312		

[a] The dates for measurements of photosynthetic carbon fixation in situ.
[b] The dates for measurements of photosynthetic carbon fixation experiencing temperature and pCO_2 treatments.
[c] Mean represents the average of daytime mean solar radiation over seven or six days microcosm incubation.

concentration was determined with a fluorometer (Trilogy, Turner Designs, USA), following the protocol of Welschmeyer (1994). The concentrations of chl *a* in situ and in microcosms were measured at the beginning and end of the experiment, respectively.

2.5. Primary productivity and dark respiration

Seawater samples taken from each microcosm at the end of the experiment were dispensed into 50 mL quartz tubes, inoculated with 5 μCi (0.185 MBq) $NaH^{14}CO_3$ (ICN Radiochemicals, USA) and then incubated for 12 h (from 6:00 a.m. to 6:00 p.m.) and 24 h (from 6:00 a.m. to 6:00 a.m. next day) under natural light and day-night conditions. The incubation temperature of every treatment was the same as the corresponding microcosm treatment. After the incubation, the cells were filtered onto a Whatman GF/F glass fiber filter (25 mm), which was immediately frozen and stored at −20 °C for later analysis. In the laboratory, each frozen filter was placed into a 20 mL scintillation vial, exposed to HCl fumes overnight, and dried (55 °C, 6 h) to expel non-fixed ^{14}C. Then 3 mL scintillation cocktail (Perkin Elmer®) was added to each vial and incorporated radioactivity was counted by a liquid scintillation counting (LS 6500, Beckman Coulter, USA). The daytime primary productivity (DPP) was defined as the amount of carbon fixation during 12 h incubation. The dark respiration was defined as the difference in amount of carbon fixation between 12 h and 24 h. Carbon fixation over 24 h was taken as daily net primary productivity (NPP). Ratio of respiration to photosynthesis (R/P) was expressed as that of respiratory carbon loss to daytime carbon fixation. The primary productivity and dark respiration in situ were measured at the beginning of the experiment.

2.6. Statistical analyses

Results were expressed as means of replicates ± standard deviation. Data were analyzed using the software SPSS v.21. The data from each treatment conformed to a normal distribution (Shapiro-Wilk, $P > 0.05$) and the variances could be considered equal (Levene's test, $P > 0.05$). One-way ANOVAs were conducted to assess the significant differences in carbonate chemistry parameters, chl *a*, DPP, NPP, dark respiration, ratio of dark respiration to photosynthesis between three treatments. Tukey HSD was conducted for post hoc investigation. Independent samples *t*-tests were conducted to compare in situ chl *a*, DPP, NPP, dark respiration, and ratio of dark respiration to photosynthesis between both stations. The threshold value for determining statistical significance was $P < 0.05$.

3. Results

The incident solar radiation during the experiment was recorded (Table 1). The daytime (12 h) mean solar radiation ranged from 927 to 1592 μmol photons m^{-2} s^{-1} at station SEATS while the lowest solar radiance was only 111 μmol photons m^{-2} s^{-1}, with the highest of 1583 μmol photons m^{-2} s^{-1}, at station D001. The average of daytime mean solar radiation over the microcosm incubation at station SEATS was 16% higher than that at station D001.

The changes of the seawater carbonate system under different conditions are shown in Table 2. At station SEATS, an increase of 3 °C in temperature (HTLC) did not alter carbonate parameters except leading to enhanced CO_3^{2-} (Tukey HSD, $P = 0.009$). HTHC resulted in a significant decrease in CO_3^{2-} (Tukey HSD, $P < 0.001$) and TA (Tukey HSD, $P = 0.016$) but an increase in CO_2 (Tukey HSD, $P < 0.001$) compared with LTLC. The effect of temperature on carbonate parameters at station D001 were similar to station SEATS, while HTHC increased HCO_3^- (Tukey HSD, $P = 0.046$) and did not affect TA (Tukey HSD, $P = 0.203$).

The in situ chl *a* levels at station SEATS and station D001 were 0.15 ± 0.02 μg L^{-1} and 0.37 ± 0.05 μg L^{-1} (Fig. 2a), respectively. After seven days incubation in the microcosms at station SEATS, Tukey comparison ($P = 0.05$) showed that higher temperature (0.46 ± 0.04 μg L^{-1}) increased chl *a* compared with LTLC (0.23 ± 0.03 μg L^{-1}) while HTHC (0.07 ± 0.01 μg L^{-1}) reduced it (Fig. 2b). The higher temperature (0.72 ± 0.07 μg L^{-1}) also increased chl *a* compared with LTLC (0.41 ± 0.05 μg L^{-1}) at station D001 (Tukey HSD, $P = 0.001$; Fig. 2b), but with no effect of HTLC (0.41 ± 0.04 μg L^{-1}) (Tukey HSD, $P = 0.988$).

The in situ DPP at station D001 (49.4 ± 4.5 μg C L^{-1} d^{-1} or 133.4 ± 12.1 μg C (μg chl *a*)$^{-1}$ d^{-1}) was dramatically higher than that at station SEATS (5.1 ± 0.5 μg C L^{-1} d^{-1} or 34.1 ± 3.1 μg C (μg chl *a*)$^{-1}$ d^{-1}), whether normalized to volume of seawater (Independent samples *t*-test, $t = -17.056$, df = 4, $P < 0.001$; Fig. 3a) or chl *a* (Independent samples *t*-test, $t = -13.786$, df = 4, $P < 0.001$; Fig. 3b). After seven days incubation in microcosms, the DPP normalized to volume of seawater under HTLC (33.2 ± 4.8 μg C L^{-1} d^{-1}) at station SEATS was significantly higher than that under LTLC (9.9 ± 1.2 μg C L^{-1} d^{-1}) and HTHC (6.6 ± 0.6 μg C L^{-1} d^{-1}) (Tukey HSD, $P < 0.001$) while the difference between LTLC and HTHC was insignificant (Tukey HSD, $P = 0.380$; Fig. 3c). The pattern at station D001 was similar to SEATS (Fig. 3c). When DPP was

Table 2
Parameters of the seawater carbonate system at different incubation conditions. Measurements and estimation of the parameters were described in Methods. Data are the means ± SD ($n = 3$). LTLC, low temperature and low pCO_2; HTLC, high temperature and low pCO_2; HTHC, high temperature and high pCO_2. DIC = dissolved inorganic carbon, TA = total alkalinity. Different superscript letters indicate significant differences among treatments within one station.

	SEATS			D001		
	LTLC	HTLC	HTHC	LTLC	HTLC	HTHC
Temperature (°C)	30.5 ± 1.0	33.5 ± 1.0	33.5 ± 1.0	28.5 ± 1.0	31.5 ± 1.0	31.5 ± 1.0
pH_T	8.07 ± 0.01	8.05 ± 0.01	7.68 ± 0.01	8.02 ± 0.01	8.01 ± 0.01	7.68 ± 0.01
pCO_2 (μatm)	390.0 ± 19.5	390.0 ± 19.5	1000.0 ± 70.0	420.0 ± 25.2	420.0 ± 25.2	1030.0 ± 60.0
DIC (μmol kg^{-1})	2056.4 ± 49.2^{a}	1986.6 ± 47.1^{a}	1999.9 ± 91.4^{a}	1969 ± 67.7^{A}	1896.5 ± 64.8^{A}	2039.1 ± 69.5^{A}
HCO_3^- (μmol kg^{-1})	1758.4 ± 47.5^{ab}	1681.2 ± 45.4^{a}	1838.4 ± 86.5^{b}	1719.2 ± 63.7^{A}	1640.9 ± 60.7^{A}	1882.3 ± 66.4^{B}
CO_3^{2-} (μmol kg^{-1})	288.2 ± 1.2^{b}	296.2 ± 1.2^{c}	138.1 ± 3.3^{a}	238.8 ± 3.4^{B}	245.3 ± 3.5^{B}	131.6 ± 1.7^{A}
CO_2 (μmol kg^{-1})	9.8 ± 0.5^{a}	9.1 ± 0.5^{a}	23.5 ± 1.7^{b}	11.0 ± 0.7^{A}	10.3 ± 0.7^{A}	25.2 ± 1.5^{B}
TA (μmol kg^{-1})	2443.5 ± 47.9^{a}	2387.7 ± 45.8^{a}	2170.7 ± 92.0^{b}	2294.2 ± 68.6^{A}	2260.0 ± 33.9^{A}	2199.4 ± 68.5^{B}

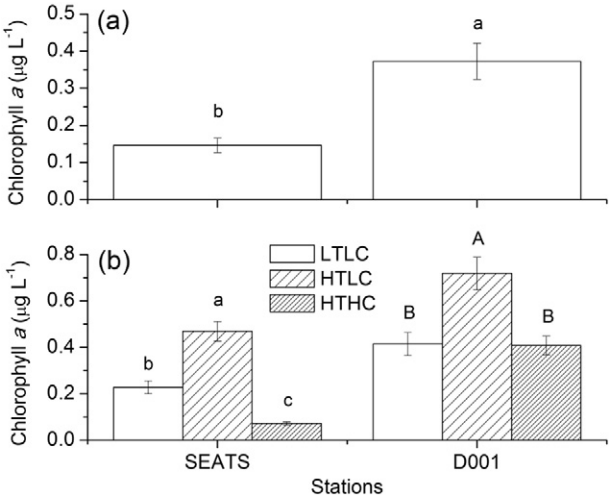

Fig. 2. Chl *a* concentration in situ (a) and after temperature and pCO_2 treatments in microcosms (b). The microcosm incubations lasted seven days at off-shore station SEATS and six days at near-shore station D001. The error bars indicate the standard deviations ($n = 3$). The different letters above the error bars represent significant ($P < 0.05$) differences between stations in panel (a) and among treatments within one station in panel (b).

normalized to chl *a*, the higher temperature increased primary productivity from 43.2 ± 5.1 to 70.7 ± 10.1 μg C (μg chl *a*)$^{-1}$ d^{-1} (Tukey HSD, $P = 0.014$) and further to 93.9 ± 8.1 μg C (μg chl *a*)$^{-1}$ d^{-1} (Tukey HSD, $P < 0.001$) when higher CO_2 was combined at station SEATS (Fig. 3d). In contrast, temperature did not affect DPP (Tukey HSD, $P = 0.0924$) and HTHC reduced it from 150.3 ± 4.9 to 128.0 ± 11.5 μg C (μg chl *a*)$^{-1}$ d^{-1} (Tukey HSD, $P = 0.039$) at station D001 (Fig. 3d).

The in situ NPP at stations SEATS and D001 were 3.5 ± 0.1 μg C L^{-1} d^{-1} (23.2 ± 1.0 μg C (μg chl *a*)$^{-1}$ d^{-1}) and 37.4 ± 3.1 μg C L^{-1} d^{-1} (91.2 ± 7.5 μg C (μg chl *a*)$^{-1}$ d^{-1}) respectively, which indicates that station D001 has higher NPP, irrespective of normalizing to volume of seawater (Independent samples *t*-test, $t = -18.998$, df = 4, $P < 0.001$; Fig. 4a) or chl *a* (Independent samples *t*-test, $t = -15.511$, df = 4, $P < 0.001$; Fig. 4b). After a seven-day incubation in the microcosms, the higher temperature increased NPP to 23.9 ± 5.3 μg C L^{-1} d^{-1} (Tukey HSD, $P = 0.001$) while HTHC (5.5 ± 0.4 μg C L^{-1} d^{-1}) did not change it (Tukey HSD, $P = 0.793$) compared with LTLC (7.2 ± 0.8 μg C L^{-1} d^{-1}) (Fig. 4c). The effects of temperature and CO_2 on NPP at station D001 were similar to that at station SEATS. When NPP was normalized to chl *a*, the higher temperature increased NPP from 31.1 ± 3.5 to 50.9 ± 11.3 (Tukey HSD, $P = 0.044$) and further to 78.3 ± 5.9 μg C (μg chl *a*)$^{-1}$ d^{-1} with the addition of higher CO_2 (Tukey HSD, $P < 0.001$) at station SEATS (Fig. 4d). On the other hand, neither HT (Tukey HSD, $P = 0.707$) nor HTHC (Tukey HSD, $P = 0.057$) affected NPP at station D001.

The in situ dark respiration rate at station SEATS was remarkably lower than that at station D001 regardless of normalizing to volume of seawater (Independent samples *t*-test, $t = -11.568$, df = 4, $P < 0.001$; Fig. 5a) or chl *a* (Independent samples *t*-test, $t = -8.019$, df = 4, $P = 0.001$; Fig. 5b). The higher temperature increased dark respiration rate from 2.8 ± 1.2 to 9.3 ± 0.6 μg C L^{-1} d^{-1} (Tukey HSD, $P < 0.001$) at station SEATS while HTHC reduced it to 1.1 ± 0.2 μg C L^{-1} d^{-1} (Tukey HSD, $P = 0.009$; Fig. 5c). The higher temperature also promoted dark respiration rate at station D001, from 16.9 ± 2.0 to 31.5 ± 5.1 μg C L^{-1} d^{-1} (Tukey HSD, $P = 0.007$) but HTHC did not alter it (Tukey HSD, $P = 0.516$; Fig. 5c). When it was normalized to chl *a*, higher temperature still increased dark respiration rate from 12.0 ± 1.8 to 19.7 ± 1.4 μg C (μg chl *a*)$^{-1}$ d^{-1} (Tukey HSD, $P = 0.006$) while the effect of temperature on respiration rate at station D001 was insignificant (Tukey HSD, $P = 0.891$; Fig. 5d). Compared to LTLC, HTHC did not affect respiration rate at either station (Tukey HSD, $P = 0.131$ at station SEATS, $P = 0.348$ at station D001; Fig. 5d).

The in situ ratio of respiration to photosynthesis was 31.9 ± 3.5% at station SEATS, significantly higher than that (24.2 ± 1.3%) at station D001 (Independent samples *t*-test, $t = 3.537$, df = 4, $P = 0.0024$; Fig. 6a). After seven days incubation in microcosms, Tukey HSD comparison ($P = 0.05$) showed that higher temperature did not affect the ratio of respiration to photosynthesis but HTHC reduced it from 27.8 ± 1.6% to 16.5 ± 1.3% at station SEATS (Fig. 6b). On the contrary, HTHC (38.7 ± 3.1%) increased the ratio compared to LTLC (27.3 ± 2.4%), with insignificant effect of temperature alone (29.5 ± 3.3%) at station D001 (Fig. 6b).

4. Discussion

4.1. Effects of increased temperature and CO_2 on biomass

The higher temperature increased chl *a* concentration at both stations, which might be attributed to increased active uptake of nutrients at the elevated temperatures through enhanced enzymatic activities. Algal and cyanobacterial growth commonly increases with temperature within a suitable range and then decreases after the optimal temperature point/range (Goldman and Carpenter, 1974; Montagnes and Franklin, 2001; Savage et al., 2004; Boyd et al., 2013) and optimum temperatures for growth of marine phytoplankton are usually several degrees higher than the environmental temperatures (Thomas et al., 2012), which could explained the increase chl *a* level of phytoplankton grown at the higher temperature in the present study.

On the other hand, the elevated CO_2 offset the positive effect of the higher temperature on chl *a* at station D001, and even reduced chl *a* at station SEATS. High CO_2 can sometimes enhance algal photosynthesis and growth, since CO_2 in seawater is suboptimal for full operation of Rubisco enzymes (Giordano et al., 2005 and references therein). On the other hand, positive effects of elevated CO_2 can be affected by other environmental factors. Gao et al. (2012b) demonstrated that rising CO_2 could enhance growth of diatoms at low light intensity, but decrease it at high light intensity. It was found that rising CO_2 concentration lowered the threshold for diatom growth above which photosynthetic active radiation becomes excessive or stressful, owing to reduced energy requirements for inorganic carbon acquisition at elevated CO_2 (Gao et al., 2012b). In the present study, the mean daily solar radiation levels during incubation were 1312 and 1136 μmol photons m^{-2} s^{-1} (Table 1), corresponding to phytoplankton in the microcosms exposed to 1068–1194 μmol photons m^{-2} s^{-1} at the off-shore station SEATS and 729–1034 μmol photons m^{-2} s^{-1} at the near-shore station D001, which were above the threshold light intensity reported for diatoms (Gao et al., 2012b). Consequently, the higher CO_2 combined with the high solar radiation in summer of NSCS may have imposed negative effects on phytoplankton biomass at stations SEATS and D001. In addition, the inhibitory effect of higher CO_2 on biomass was more significant at station SEATS than D001. This can be attributed to the higher sensitivity of picoplankton to high solar radiation (Li et al., 2011; Wu et al., 2015), which could be delivered to the interaction of high solar radiation and high CO_2. As shown in Li et al.'s (2011) study, the proportion of picoplankton in phytoplankton assemblages increased with distance off the coasts. Therefore, the dominant species at station SEATS are pico- and nano-phytoplankton, but micro-phytoplankton at station D001 (Table 3).

4.2. Effects of increased levels of temperature and CO_2 on primary productivity

The seawater volume-specific DPP at station D001 was higher than station SEATS. This should result from both higher chl *a* concentration and chl *a*-specific DPP at D001. It has been shown that more smaller cells exist at SEATS than at D001 (Table 3). Smaller cells have been considered to have larger DPP, according to Laws' (1975) model. The discrepancy between our finding and Laws' model may be due to the

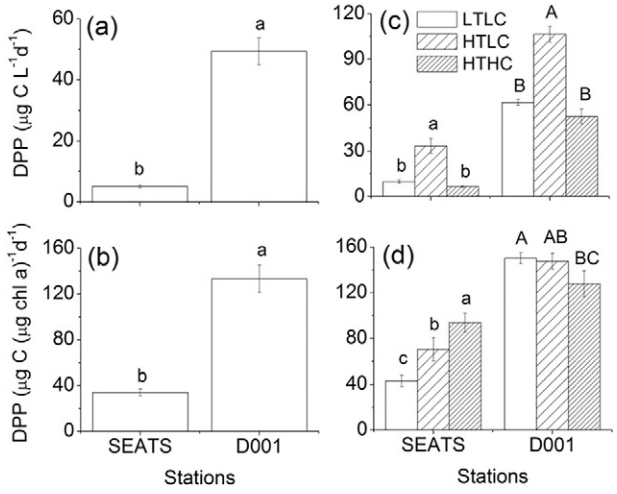

Fig. 3. Daytime primary productivity (DPP) in situ (a, b) and after temperature and pCO_2 treatments in microcosms (c, d). The microcosm incubations lasted seven days at offshore station SEATS and six days at near-shore station D001. The error bars indicate the standard deviations ($n = 3$). The different letters above the error bars represent significant ($P < 0.05$) differences between stations in panels (a, b) and among treatments within one station in panels (c, d).

availability of nutrients. Laws' model was based on growth rates obtained from the same nutrient level. Nevertheless, the nutrient level at station D001 is higher than at SEATS (Table 3), leading to higher DPP. The higher temperature increased seawater volume-specific DPP at both stations. This could be attributed to more biomass produced at the warmer conditions, as indicated by chl *a*. High temperature enhanced the chl *a*-specific DPP at station SEATS. However, no positive effects of temperature were found on chl *a*-specific DPP at station D001. The differential effects of temperature on chl *a*-specific DPP between the stations may be due to the phytoplankton community composition, since cyanobacteria and/or pico-phytoplankton have the strongest temperature response in terms of photosynthetic carbon fixation compared to micro- and nano-phytoplankton (Andersson et al., 1994). This finding contributes to the explanation of the dominance of pico-phytoplankton in a warmer ocean (Montagnes and Franklin, 2001; Hare et al., 2007; Morán et al., 2010; Chen et al., 2014). HTHC reduced chl *a*-specific DPP at station D001, but increased it at station SEATS. High CO_2 also reduced chl *a*-specific DPP in a previous study, which could result from the interaction of high CO_2 and high solar radiation during the summer in the NSCS (Gao et al., 2012b). The reason that HTHC stimulated chl *a*-specific DPP at station SEATS may be due to a dramatic decline in chl *a* concentration under the HTHC treatment.

4.3. Effects of increased temperature and CO_2 on respiration

The dark respiration rate of phytoplankton at station D001 was higher than that at SEATS, regardless of normalizing to seawater or chl *a*. The respiration rate of algae or cyanobacteria usually increases with cell size (López-Sandoval et al., 2014). Station SEATS has more pico-phytoplankton, which would lead to a lower chl *a*-specific dark respiration rate and then lower seawater volume-specific dark respiration, particularly when combined with lower chl *a* level. The higher temperature increased seawater volume-specific dark respiration at both stations, which could be related to increased chl *a* concentration and/or enhanced respiratory carbon loss at the higher temperature. The higher temperature also increased chl *a*-specific dark respiration rate at station SEATS. This is consistent with Butrón et al.'s (2009) study, in which respiration rates of phytoplankton along Nervión–Ibaizabal estuary showed a positive correlation with temperature. Robarts and Zohary (1987) also found that respiration rate of bloom-forming cyanobacteria was temperature-dependent, with optima over 25 °C. On the other hand, the higher temperature did not increase the chl *a*-specific dark respiration rate at station D001. This may be due to the lower sensitivity of larger cells to temperature changes. It has been noted that smaller algae have a significantly larger metabolic response upon exposure to higher incubation temperatures, compared to larger algae (Staehr and Birkeland, 2006).

HTHC reduced seawater volume-specific dark respiration at both stations, which should be the consequence of the decreased chl *a* in this treatment. The higher temperature increased chl *a*-specific dark respiration rate at station SEATS, but there was no significant difference between HTHC and LTLC, indicating the higher CO_2 inhibited the chl *a*-specific dark respiration rate. Similarly, reduced respiration was found in mesocosm studies (Spilling et al., 2016). In theory, higher CO_2 would inhibit respiratory release of CO_2. Nevertheless, enhanced respiration rate at higher CO_2 conditions have been commonly found in laboratory-grown diatoms (Wu et al., 2010; Yang and Gao, 2012; Li et al., 2016), coccolithophores (Jin et al., 2015), mixed phytoplankton assemblages (Jin et al., 2015), and macroalgae (Zou et al., 2011; Xu et al., 2017). Such increased respiration has been attributed to extra energy demand to cope with increased seawater acidity caused by higher CO_2 (Gao and Campbell, 2014; Raven et al., 2014). Therefore, the effect of increased CO_2 on phytoplankton respiration could be due to the combined effects of CO_2 diffusive resistance and seawater acidity stress. Meanwhile, HTHC did not affect chl *a*-specific dark respiration rate at station D001. One possible reason could be that larger cells are less sensitive to CO_2 diffusive resistance and acidic stress due to thicker diffusion boundary layers around the cells. This hypothetical explanation is worthy of future testing.

4.4. Effects of increased temperature and CO_2 on R/P

Laws' (1975) model suggests that large phytoplankton cells are likely to have a lower ratio of respiration to photosynthesis. This may allow them to compete with smaller phytoplankton cells in terms of the growth rate, considering small cells have higher daytime productivity. Our finding that phytoplankton station D001 had a lower R/P than station SEATS supports Laws' model. It was theorized that autotrophic respiration is more sensitive to temperature than photosynthesis and the ratio of R/P was predicted to increase with temperature (Woodwell et al., 1983; Woodwell, 1990). However, the assumption that plant respiration is highly temperature dependent was primarily based on short-

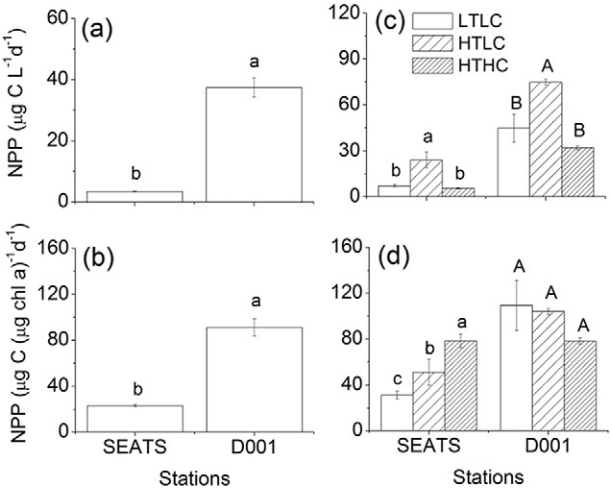

Fig. 4. Net primary productivity (NPP) in situ (a, b) and after temperature and pCO_2 treatments in microcosms (c, d). The microcosm incubations lasted seven days at offshore station SEATS and six days at near-shore station D001. The error bars indicate the standard deviations ($n = 3$). The different letters above the error bars represent significant ($P < 0.05$) differences between stations in panels (a, b) and among treatments within one station in panels (c, d).

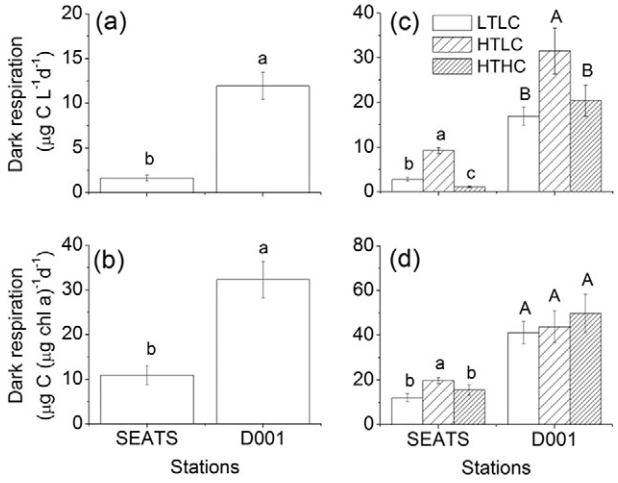

Fig. 5. Dark respiration in situ (a, b) and after temperature and pCO_2 treatments in microcosms (c, d). The microcosm incubations lasted seven days at off-shore station SEATS and six days at near-shore station D001. The error bars indicate the standard deviations ($n = 3$). The different letters above the error bars represent significant ($P < 0.05$) differences between stations in panels (a, b) and among treatments within one station in panels (c, d).

term (a few minutes or hours) responses of plants to changes of temperature (Gifford, 1994). In long-term experiments (days or months), the increase in respiration with temperature tends to be lost partially or even disappear completely, depending on the degree of acclimation (Jones, 1977; Gifford, 1995; Ziska and Bunce, 1998; Slot and Kitajima, 2015; Reich et al., 2016). Photosynthetic acclimation to warming is variable (Hancke and Glud, 2004; Staehr and birkeland 2006; Chalifour and Juneau, 2011; Schlüter et al., 2014). However, a general acclimation response to long-term increased temperature is a rise in the optimal temperature of photosynthesis (Staehr and Birkeland, 2006; Kattge and Knorr, 2007; Gunderson et al., 2010). Such shifts in the temperature response of photosynthesis and respiration via physiological acclimation can dampen the increase in R/P at high temperatures, or climate warming would not increase R/P (Drake et al., 2016; Reich et al., 2016). In other words, phytoplankton would down-regulate the high sensitivity of respiration to temperature, and maintain a relatively

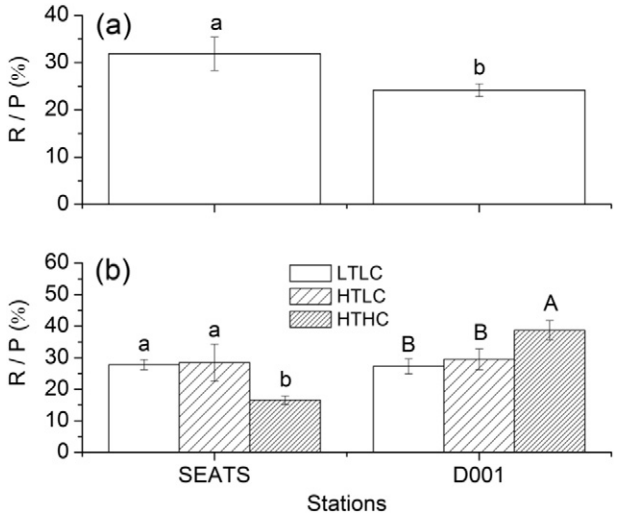

Fig. 6. The ratio of respiration to photosynthesis in situ (a, b) and after temperature and pCO_2 treatments (c, d) in microcosms. The microcosm incubations lasted seven days at off-shore station SEATS and six days at near-shore station D001. The error bars indicate the standard deviations ($n = 3$). The different letters above the error bars represent significant ($P < 0.05$) differences between stations in panels (a, b) and among treatments within one station in panels (c, d).

Table 3
Physical, chemical, and biological parameters at off-shore station SEATS and near-shore station D001. SST: seawater surface temperature; N: $NO_3^- + NO_2^-$ (μmol L^{-1}); P: PO_4^{3-} (μmol L^{-1}). Data of nutrients and phytoplankton composition are derived from literatures.

Station	SST	Salinity	pH_T	N	P	Dominant phytoplankton
SEATS	28.7	32.9	8.07	<0.1[a]	<0.01[b]	Pico- and nano-phytoplankton[c]
D001	26.8	33.5	8.03	>1[d]	>0.1[d]	Micro-phytoplankton[e]

[a] Du et al. (2013).
[b] Wu et al. (2003).
[c] Li et al. (2011).
[d] Li et al. (2014).
[e] Zhang et al. (2014).

consistent net primary production and hence food web structure in a warming ocean. The ratio of R/P did not vary with increased temperature at either station in our work either, although both photosynthesis and respiration were enhanced by the higher temperature. Our finding indicates that an incubation period of 6–7 days could result in a partial acclimation for phytoplankton assemblages to increased temperature in the SCS, but is not long enough for their complete acclimation. Therefore, the stimulatory effects of high temperature on photosynthesis and respiration were still notable. In addition, opposite effects of HTHC on R/P were detected at stations SEATS and D001, negative at SEATS and positive at D001. This can be attributed to differential responses of photosynthesis at both stations to HTHC, considering the responses of respiration were similar.

5. Conclusions

This study demonstrates that short term rise of SST appeared to simulate the biomass, primary productivity, and dark respiration of phytoplankton assemblages in NSCS. However, this positive effect could be dampened or offset when warming and ocean acidification treatments were combined. The regional responses of phytoplankton assemblages at the two stations to ocean warming and acidification may differ due to differences in physical and chemical environment as well as phytoplankton community structure. The combined treatment of warming and acidification reduced biomass and dark respiration rate at the off-shore station but did not affect them at the near-shore station. It seems that phytoplankton assemblages in pelagic areas are more sensitive to ocean warming and acidification. Ecologically and geographically, our data implies differential responses of primary production to ocean climate change.

Supplementary data to this article can be found online at http://dx.doi.org/10.1016/j.marpolbul.2017.02.063.

Acknowledgements

This study was supported by National Natural Science Foundation (41430967; 41120164007), State Oceanic Administration (National Programme on Global Change and Air-Sea Interaction, GASI-03-01-02-04), the Science Foundation of Huaihai Institute of Technology (Z2016007), and the Open Project Program of Marine Resources Development Institute of Jiangsu (JSIMR201601).

References

Andersson, A., Haecky, P., Hagström, Å., 1994. Effect of temperature and light on the growth of micro-nano-and pico-plankton: impact on algal succession. Mar. Biol. 120, 511–520.

Boyd, P.W., Rynearson, T.A., Armstrong, E.A., Fu, F., Hayashi, K., Hu, Z., Hutchins, D.A., Kudela, R.M., Litchman, E., Mulholland, M.R., Passow, U., Strzepek, R.F., Whittaker, K.A., Yu, E., Thomas, M.K., 2013. Marine phytoplankton temperature versus growth responses from polar to tropical waters — outcome of a scientific community-wide study. PLoS One 8, e63091.

Butrón, A., Iriarte, A., Madariaga, I., 2009. Size-fractionated phytoplankton biomass, primary production and respiration in the Nervión–Ibaizabal estuary: a comparison with other nearshore coastal and estuarine ecosystems from the Bay of Biscay. Cont. Shelf Res. 29, 1088–1102.

Chalifour, A., Juneau, P., 2011. Temperature-dependent sensitivity of growth and photosynthesis of *Scenedesmus obliquus*, *Navicula pelliculosa* and two strains of *Microcystis aeruginosa* to the herbicide atrazine. Aquat. Toxicol. 103, 9–17.

Chen, B., Liu, H., Huang, B., Wang, J., 2014. Temperature effects on the growth rate of marine picoplankton. Mar. Ecol. Prog. Ser. 505, 37–47.

Drake, J.E., Tjoelker, M.G., Aspinwall, M.J., Reich, P.B., Barton, C.V.M., Medlyn, B.E., Duursma, R.A., 2016. Does physiological acclimation to climate warming stabilize the ratio of canopy respiration to photosynthesis? New Phytol. 211, 850–863.

Du, C., Liu, Z., Dai, M., Kao, S.-J., Cao, Z., Zhang, Y., Huang, T., Wang, L., Li, Y., 2013. Impact of the Kuroshio intrusion on the nutrient inventory in the upper northern South China Sea: insights from an isopycnal mixing model. Biogeosciences 10, 6419–6432.

Falkowski, P.G., Raven, J.A., 2013. Aquatic Photosynthesis. Princeton University Press, USA.

Fang, G., Chen, H., Wei, Z., Wang, Y., Wang, X., Li, C., 2006. Trends and interannual variability of the South China Sea surface winds, surface height, and surface temperature in the recent decade. J. Geophys. Res. 111, 2209–2223.

Feng, Y., Hare, C.E., Leblanc, K., Rose, J.M., Zhang, Y., DiTullio, G.R., Lee, P.A., Wilhelm, S.W., Rowe, J.M., Sun, J., Nemcek, N., Gueguen, C., Passow, U., Benner, I., Brown, C., Hutchins, D.A., 2009. Effects of increased pCO_2 and temperature on the North Atlantic spring bloom. I. The phytoplankton community and biogeochemical response. Mar. Ecol. Prog. Ser. 388, 13–25.

Gao, K., Campbell, D., 2014. Photophysiological responses of marine diatoms to elevated CO_2 and decreased pH: a review. Funct. Plant Biol. 41, 449–459.

Gao, K., Helbling, E.W., Häder, D.-P., Hutchins, D.A., 2012a. Responses of marine primary producers to interactions between ocean acidification, solar radiation, and warming. Mar. Ecol. Prog. Ser. 470, 167–189.

Gao, K., Xu, J., Gao, G., Li, Y., Hutchins, D.A., Huang, B., Wang, L., Zheng, Y., Jin, P., Cai, X., 2012b. Rising CO_2 and increased light exposure synergistically reduce marine primary productivity. Nat. Clim. Chang. 2, 519–523.

Gifford, R., 1994. The global carbon cycle: a viewpoint on the missing sink. Funct. Plant Biol. 21, 1–15.

Gifford, R.M., 1995. Whole plant respiration and photosynthesis of wheat under increased CO_2 concentration and temperature: long-term vs. short-term distinctions for modelling. Glob. Change Biol. 1, 385–396.

Giordano, M., Beardall, J., Raven, J.A., 2005. CO_2 concentrating mechanisms in algae: mechanisms, environmental modulation, and evolution. Annu. Rev. Plant Biol. 56, 99–131.

Goldman, J.C., Carpenter, E.J., 1974. A kinetic approach to the effect of temperature on algal growth. Limnol. Oceanogr. 19, 756–766.

Gunderson, C.A., O'hara, K.H., Campion, C.M., Walker, A.V., Edwards, N.T., 2010. Thermal plasticity of photosynthesis: the role of acclimation in forest responses to a warming climate. Glob. Chang. Biol. 16, 2272–2286.

Häder, D.-P., Gao, K., 2015. Interactions of anthropogenic stress factors on marine phytoplankton. Front. Environ. Sci. 3, 14.

Hancke, K., Glud, R.N., 2004. Temperature effects on respiration and photosynthesis in three diatom-dominated benthic communities. Aquat. Microb. Ecol. 37, 265–281.

Hare, C.E., Leblanc, K., DiTullio, G.R., Kudela, R.M., Zhang, Y., Lee, P.A., Riseman, S., Tortell, P.D., Hutchins, D.A., 2007. Consequences of increased temperature and CO_2 for algal community structure and biogeochemistry in the Bering Sea. Mar. Ecol. Prog. Ser. 352, 9–16.

Hein, M., Sand-Jensen, K., 1997. CO_2 increases oceanic primary production. Nature 388, 526–527.

Holding, J., Duarte, C., Sanz-Martín, M., Mesa, E., Arrieta, J., Chierici, M., Hendriks, I., García-Corral, L., Regaudie-de-Gioux, A., Delgado, A., 2015. Temperature dependence of CO_2-enhanced primary production in the European Arctic Ocean. Nat. Clim. Chang. 5, 1079–1082.

IPCC, 2013. Climate change 2013: the physical science basis. In: Stocker, T.F., Qin, D., Plattner, G.-K., Tignor, M., Allen, S.K., Boschung, J., Nauels, A., Xia, Y., Bex, V., Midgley, P.M. (Eds.), Working Group I Contribution to the Fifth Assessment Report of the Intergovernmental Panel on Climate Change. Cambridge Univ. Press, New York.

Jin, P., Wang, T., Liu, N., Dupont, S., Beardall, J., Boyd, P.W., Riebesell, U., Gao, K., 2015. Ocean acidification increases the accumulation of toxic phenolic compounds across trophic levels. Nat. Commun. 6:8714. http://dx.doi.org/10.1038/ncomms9714.

Jones, R.I., 1977. The importance of temperature conditioning to the respiration of natural phytoplankton communities. Br. Phycol. J. 12, 277–285.

Kattge, J., Knorr, W., 2007. Temperature acclimation in a biochemical model of photosynthesis: a reanalysis of data from 36 species. Plant Cell Environ. 30, 1176–1190.

López-Sandoval, D.C., Rodríguez-Ramos, T., Cermeño, P., Sobrino, C., Marañón, E., 2014. Photosynthesis and respiration in marine phytoplankton: relationship with cell size, taxonomic affiliation, and growth phase. J. Exp. Mar. Bio. Ecol. 457, 151–159.

Laws, E.A., 1975. The importance of respiration losses in controlling the size distribution of marine phytoplankton. Ecology 419-426, 1975.

Lewandowska, A.M., Breithaupt, P., Hillebrand, H., Hoppe, H.-G., Jürgens, K., Sommer, U., 2012. Responses of primary productivity to increased temperature and phytoplankton diversity. J. Sea Res. 72, 87–93.

Li, F., Wu, Y., Hutchins, D.A., Fu, F., Gao, K., 2016. Physiological responses of coastal and oceanic diatoms to diurnal fluctuations in seawater carbonate chemistry under two CO_2 concentrations. Biogeosciences 13, 6247–6259.

Li, G., Gao, K., Gao, G., 2011. Differential impacts of solar UV radiation on photosynthetic carbon fixation from the coastal to offshore surface waters in the South China Sea. Photochem. Photobiol. 87, 329–334.

Li, R.H., Liu, S.M., Li, Y.W., Zhang, G.L., Ren, J.L., Zhang, J., 2014. Nutrient dynamics in tropical rivers, lagoons, and coastal ecosystems of eastern Hainan Island, South China Sea. Biogeosciences 11, 481–506.

Liu, Y., Peng, Z., Zhou, R., Song, S., Liu, W., You, C.F., Lin, Y.P., Yu, K., Wu, C.C., Wei, G., 2014. Acceleration of modern acidification in the South China Sea driven by anthropogenic CO_2. Sci. Rep. 4, 1158–1159.

Montagnes, D.J., Franklin, M., 2001. Effect of temperature on diatom volume, growth rate, and carbon and nitrogen content: reconsidering some paradigms. Limnol. Oceanogr. 46, 2008–2018.

Morán, X.A.G., López-Urrutia, Á., Calvo-Díaz, A., Li, W.K., 2010. Increasing importance of small phytoplankton in a warmer ocean. Glob. Chang. Biol. 16, 1137–1144.

Mostofa, K.M., Liu, C., Zhai, W., Minella, M., Vione, D., Gao, K., Minakata, D., Arakaki, T., Yoshioka, T., Hayakawa, K., Konohira, E., Tanoue, D., Akhand, A., Chanda, A., Wang, B., Sakugawa, H., 2016. Reviews and syntheses: ocean acidification and its potential impacts on marine ecosystems. Biogeosciences 13, 1767–1786.

Orr, J.C., Fabry, V.J., Aumont, O., Bopp, L., Doney, S.C., Feely, R.A., Gnanadesikan, A., Gruber, N., Ishida, A., Joos, F., 2005. Anthropogenic ocean acidification over the twenty-first century and its impact on calcifying organisms. Nature 437, 681–686.

Pierrot, D., Lewis, E., Wallace, D.W.R., 2006. MS Excel Program Developed for CO_2 System Calculations, ORNL/CDIAC-105a. Carbon Dioxide Information Analysis Center, Oak Ridge National Laboratory, US Department of Energy, Oak Ridge, Tennessee.

Poll, W., Kulk, G., Timmermans, K., Brussaard, C., Woerd, H., Kehoe, M., Mojica, K., Visser, R., Rozema, P., Buma, A., 2013. Phytoplankton chlorophyll *a* biomass, composition, and productivity along a temperature and stratification gradient in the northeast Atlantic Ocean. Biogeosciences 10, 4227–4240.

Raven, J., 1993. Limits on growth rates. Nature 361, 209–210.

Raven, J.A., Beardall, J., Giordano, M., 2014. Energy costs of carbon dioxide concentrating mechanisms in aquatic organisms. Photosynth. Res. 121, 111–124.

Raven, J.A., Giordano, M., Beardall, J., Maberly, S.C., 2012. Algal evolution in relation to atmospheric CO_2: carboxylases, carbon-concentrating mechanisms and carbon oxidation cycles. Phil. Trans. R. Soc. B 367, 493–507.

Reich, P.B., Sendall, K.M., Stefanski, A., Wei, X., Rich, R.L., Montgomery, R.A., 2016. Boreal and temperate trees show strong acclimation of respiration to warming. Nature 531, 633–636.

Reinfelder, J.R., 2011. Carbon concentrating mechanisms in eukaryotic marine phytoplankton. Annu. Rev. Mar. Sci. 3, 291–315.

Riebesell, U., Wolf-Gladrow, D., Smetacek, V., 1993. Carbon dioxide limitation of marine phytoplankton growth rates. Nature 361, 249–251.

Robarts, R.D., Zohary, T., 1987. Temperature effects on photosynthetic capacity, respiration, and growth rates of bloom-forming cyanobacteria. N. Z. J. Mar. Freshw. Res. 21, 391–399.

Roy, R.N., Roy, L.N., Vogel, K.M., Porter-Moore, C., Pearson, T., Good, C.E., Millero, F.J., Campbell, D., 1993. M: the dissociation constants of carbonic acid in seawater at salinities 5 to 45 and temperatures 0 to 45 °C. Mar. Chem. 44, 249–267.

Savage, V.M., Gillooly, J.F., Brown, J.H., West, G.B., Charnov, E.L., 2004. Effects of body size and temperature on population growth. Am. Nat. 163, 429–441.

Schippers, P., Lürling, M., Scheffer, M., 2004. Increase of atmospheric CO_2 promotes phytoplankton productivity. Ecol. Lett. 7, 446–451.

Schlüter, L., Lohbeck, K.T., Gutowska, M.A., Groger, J.P., Riebesell, U., Reusch, T.B.H., 2014. Adaptation of a globally important coccolithophore to ocean warming and acidification. Nat. Clim. Chang. 4, 1024–1030.

Slot, M., Kitajima, K., 2015. General patterns of acclimation of leaf respiration to elevated temperatures across biomes and plant types. Oecologia 177, 885–900.

Sommer, U., Paul, C., Moustaka-Gouni, M., 2015. Warming and ocean acidification effects on phytoplankton—from species shifts to size shifts within species in a mesocosm experiment. PLoS One 10, e0125239.

Spilling, K., Paul, A.J., Virkkala, N., Hastings, T., Lischka, S., Stuhr, A., Bermudez, R., Czerny, J., Boxhammer, T., Schulz, K.G., Ludwig, A., Riebesell, U., 2016. Ocean acidification decreases plankton respiration: evidence from a mesocosm experiment. Biogeosciences 13:4707–4719. http://dx.doi.org/10.5194/bg-2015-608.

Staehr, P.A., Birkeland, M.J., 2006. Temperature acclimation of growth, photosynthesis and respiration in two mesophilic phytoplankton species. Phycologia 45, 648–656.

Thomas, M.K., Kremer, C.T., Klausmeier, C.A., Litchman, E., 2012. A global pattern of thermal adaptation in marine phytoplankton. Science 338, 1085–1088.

Tatters, A.O., Roleda, M.Y., Schnetzer, A., Fu, F.-X., Hurd, C., Boyd, P.W., Caron, D.A., Lie, A.A.Y., Hoffmann, L., Hutchins, D.A., 2013. Short-term and long-term conditioning of a temperate marine diatom community to acidification and warming. Phil. Trans. R. Soc. B 368. http://dx.doi.org/10.1098/rstb.2012.0437 (20120437).

Welschmeyer, N.A., 1994. Fluorometric analysis of chlorophyll a in the presence of chlorophyll b and pheopigments. Limnol. Oceanogr. 39, 1985–1992.

Woodwell, G.M., 1990. The effects of global warming. In: Leggett, J. (Ed.), Global Warming: The Greenpeace Report. Oxford University Press, Oxford, UK, pp. 116–132.

Woodwell, G.M., Hobbie, J., Houghton, R., Melillo, J., Moore, B., Peterson, B., Shaver, G., 1983. Global deforestation: contribution to atmospheric carbon dioxide. Science 222, 1081–1086.

Wu, J., Chung, S., Wen, L., Liu, K., Chen, Y., Chen, H., Karl, D., 2003. Dissolved inorganic phosphorus, dissolved iron, and *Trichodesmium* in the oligotrophic South China Sea. Glob. Biogeochem. Cycles 17:1008. http://dx.doi.org/10.1029/2002GB001924.

Wu, Y., Gao, K., 2010. Combined effects of solar UV radiation and CO_2-induced seawater acidification on photosynthetic carbon fixation of phytoplankton assemblages in the South China Sea. Chin. Sci. Bull. 55, 3680–3686.

Wu, Y., Gao, K., Riebesell, U., 2010. CO_2-induced seawater acidification affects physiological performance of the marine diatom *Phaeodactylum tricornutum*. Biogeosciences 7, 2915–2923.

Wu, Y., Li, Z., Du, W., Gao, K., 2015. Physiological response of marine centric diatoms to ultraviolet radiation, with special reference to cell size. J. Photoch. Photobio. B 153, 1–6.

Xu, Z., Gao, G., Xu, J., Wu, H., 2017. Physiological response of a golden tide alga (*Sargassum muticum*) to the interaction of ocean acidification and phosphorus enrichment. Biogeosciences 14, 671–681.

Yang, G., Gao, K., 2012. Physiological responses of the marine diatom *Thalassiosira pseudonana* to increased pCO_2 and seawater acidity. Mar. Environ. Res. 79, 142–151.

Ziska, L.H., Bunce, J.A., 1998. The influence of increasing growth temperature and CO_2 concentration on the ratio of respiration to photosynthesis in soybean seedlings. Glob. Chang. Biol. 4, 637–643.

Zhang, G., Pang, Y., Chen, S., Wu, Z., Chen, D., Wang, D., Huang, B., 2014. Study on the communities of the Netz-phytoplankton in the coastal waters of Hainan Island in the early summer. Trans. Oceanol. Limnol. 3, 97–104.

Zou, D., Gao, K., Luo, H., 2011. Short- and long-term effects of elevated CO_2 on photosynthesis and respiration in the marine macroalga *Hizikia fusiformis* (Sargassaceae, Phaeophyta) grown at low and high N supplies. J. Phycol. 47, 87–97.